Available online at www.sciencedirect.com
ScienceDirect
International Journal of Heat and Mass Transfer 50 (2007) 4089–4097
International Journal of HEAT and MASS TRANSFER
www.elsevier.com/locate/ijhmt

Spray cooling on micro structured surfaces

Christof Sodtke, Peter Stephan *

Chair of Technical Thermodynamics, Darmstadt University of Technology, Petersenstrasse 30, 64287 Darmstadt, Germany

Received 5 July 2006
Available online 26 April 2007

Abstract

Spray cooling experiments have been performed on a smooth heater surface. The working fluid water was atomized through a full cone nozzle into a low pressure spray chamber. Different coolant mass fluxes were studied by varying the distance between nozzle and heater. Observations obtained with an infrared camera indicated that the length of the three phase contact line increased as the heat flux in the experiments was raised. Motivated by this finding, the effect of different micro structured surfaces, which lead to an increase in the three phase contact line, on the spray cooling performance was studied. The micro structures consisted of micro pyramids with different heights. A significant enhancement in the heat transfer performance due to the surface structures could be observed, especially at low coolant fluxes.

Additionally, high spatial resolution temperature measurements on a smooth heater using thermochromic liquid crystals were obtained. These measurements indicate high local temperature gradients for a regime where the coolant film on the heater is ruptured.

Keywords: Spray cooling; Micro structures; Contact line; TLCs; Surface temperature distribution

1. Introduction

Spray cooling is a very efficient means for dissipating high heat fluxes with low coolant mass fluxes at low wall superheats. It is used in a wide range of applications from metal quenching over cooling of high power electronics to medical treatments. Using water as coolant, spray cooling heat fluxes up to 1000 W/cm^2 have been reported [1]. Depending on the spray parameters and surface properties, the coolant forms a cohesive or ruptured thin liquid film, which evaporates on the hot surface. With decreasing film thickness the transferred heat flux at a given surface temperature increases [1].

Generally, sprays can are generated in different ways, most frequently used are pressure and air blast atomizers. In a pressure atomizer, only one phase is used for the atomizing and the subsequent cooling. In the case of a air blast atomizer, the mass flow rate of the liquid coolant is usually small compared to that of the air. Pressure atomizers are conveniently used in closed systems. The advantage of air atomizers is that they can work with lower liquid coolant flow rates.

Three different regimes can be determined in spray cooling heat transfer [2], first a low temperature regime, where liquid evaporates at the free liquid–vapour interface, second a high temperature regime, where liquid films are in a film-boiling-like state and vapour bubbles are generated at the superheated hot wall. The third regime is the transition regime from the low temperature to the high temperature region. In his experiments Toda [2] observed that subcooling had only minor effects on single phase and nucleate boiling heat transfer. A dominant effect on CHF was also not observed.

Several studies were performed on the influence of the spray parameters on the cooling heat flux, it was found that the volumetric spray flux has a dominant effect on the heat transfer [3,4] compared to other hydrodynamic parameters of the spray. Pautsch et al. [5] found that if a pressure

* Corresponding author. Tel.: +49 0 6151 16 3159; fax: +49 0 6151 16 6561.
E-mail address: pstephan@ttd.tu-darmstadt.de (P. Stephan).

0017-9310/$ - see front matter © 2007 Elsevier Ltd. All rights reserved.
doi:10.1016/j.ijheatmasstransfer.2006.12.037

Nomenclature

d_{10}	average droplet diameter (μm)
$\dot{m}$	mass flux (kg/h)
p	pressure (bar)
$\dot{q}$	heat flux (W/cm^2)
R_a	surface roughness (μm)
t	temperature (°C)
Δt	temperature difference (K)
λ	thermal conductivity (W/(m K))
τ	time constant (s)

Subscripts

con	experimental container
cyl	heater
res	reservoir
w	wall

atomizer is used, the film thickness decreases with increasing flow rate, while Yang et al. [6] found that for an air atomizer the coolant flow rate has only little effect on the film thickness.

Sehmbey et al. [7] studied the effect of surface properties on the cooling heat flux using air atomized nozzles. They found that a higher surface roughness decreases the cooling performance of the spray, due to an increased film thickness. Hsieh and Yao [8] conducted experiments studying the influence of surface micro structures on silicon wavers on the spray cooling heat flux using a pressure atomizer nozzle. Their results show an increased heat flux on structured surfaces due to capillary forces of the surface acting on the film. Smaller structures resulted in a better heat transfer. However, the improvement in heat transfer is lower than the increase in surface area. Silk et al. [9] studied the effect of cubic fins, pyramids and straight fins on the heat transfer performance up to CHF. They found that all surfaces tested improved the heat transfer performance compared to a flat surface, the straight fins performed best, followed by cubic fins and pyramids. The straight fins resulted in a ≈50% higher CHF value compared to that of a flat surface. Investigating also the influence of dissolved gas, Silk et al. [9] found the magnitude of the improvement was lower for the case of a not degassed fluid.

Recently, Horacek et al. [10] performed a study on the basic heat transfer mechanisms of spray cooling using a transparent microheater array consisting of 96 square heating elements, each having an edge length of 100 μm. They found that apparently dry spots appear in the otherwise cohesive liquid film covering the cooled surface at wall superheats in excess of 10 °C. According to [10], the heat flux is directly related to the contact line length of the three phases gas–liquid–solid and not to the wetted area.

There is some discussion about the temperature variations encountered on a spray cooled surface. While Gu et al. [11] found that compared to other cooling techniques, e.g., jet cooling, spray cooling results in a relatively uniform temperature distribution over the cooled surface, Shedd and Pautsch [12] found quite significant temperature variations over their test heater reaching as high as 17 °C.

Despite the advantages of spray cooling over competing cooling techniques, there is a reluctance to incorporate spray cooling in demanding cooling situations, which is attributed to the very limited understanding of the heat transfer mechanisms and practical concerns such as the limited repeatability of cooling performance for seemingly identical spray nozzles [13].

For the present work experiments were conducted to study the effect of surface structures and coolant mass flux on the heat transfer in the low surface temperature regime at low system pressures. Additionally, the influence of the coolant behavior on the heat transfer performance was investigated by observing the heater surface with a high-speed infrared camera and performing high resolution temperature measurements on a thin spray cooled foil heater. In the following section, the experimental set-up is described, in Section 3 experimental results are presented and discussed.

2. Experimental set-up and procedure

2.1. Experimental set-up

A schematic of the experimental set-up used is shown in Fig. 1. A Plexiglas spray chamber was constructed, which allows spray cooling at system pressures as low as 0.005 bar. The spray is generated using deionised water, a gear pump and a full cone pressure atomizer (Spraying Systems, TG SS 0.3). A heat exchanger inside the spray chamber ensures constant temperature for all experiments ($\Delta t_{con} = \pm 1$ K), independent of the ambient temperature. A second heat exchanger inside the reservoir is used to control the subcooling of the coolant ($\Delta t_{res} = \pm 0.4$ K). The coolant mass flow rate pumped through the nozzle is measured with a coriolis flow meter and can be accurately adjusted using a bypass controlled by a needle valve. A highspeed infrared imaging system (Phoenix Midas) can be used to observe the coolant distribution and behavior on the heater. Alternatively, the infrared camera can be replaced by a standard CCD-camera.

The heater surfaces are the upper end faces of differently treated copper cylinders which are placed on the bottom of the spray chamber one at a time. A fixation with a conical top ensures that excess coolant can run off towards the intercepting tank and does not accumulate on the cylinder

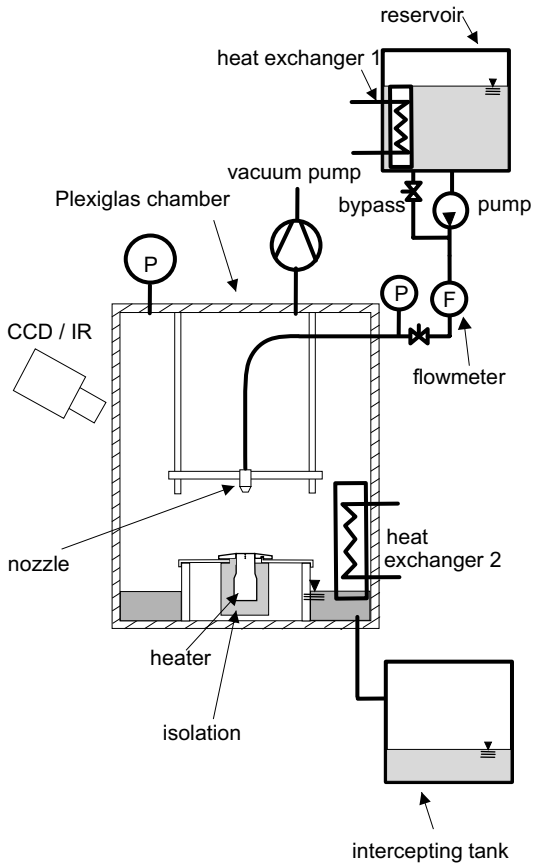

Fig. 1. Schematics of the experimental set-up.

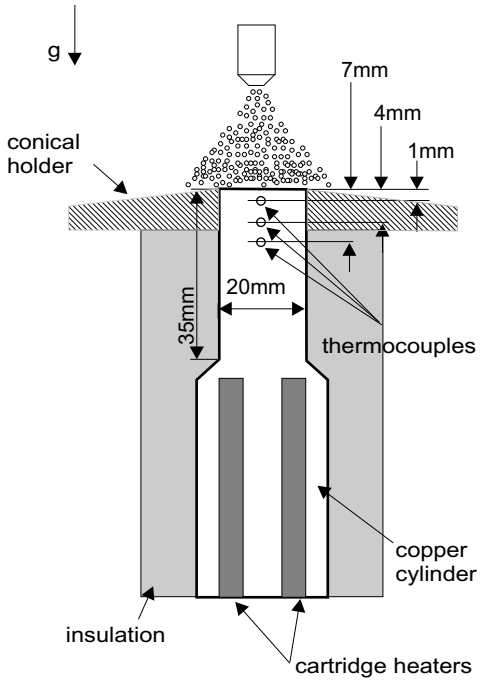

Fig. 2. Copper heater embedded in the fixation system for the spray chamber.

surface. That way, only the upper end face of the copper cylinders get in contact with the coolant and the coolant does not accumulate on the heater surface. The cylinders are electrically heated by cartridge heaters and are well insulated at the circumference. The upper end face in contact with the spray has a diameter of 20 mm. The dissipated heat flux and the surface temperature are calculated using three thermocouples spaced 3 mm apart from each other along the axis of the copper cylinder (see Fig. 2). The upper thermocouple is positioned 1 mm below the heater surface. The thermal conductivity of the copper cylinders was measured via their electrical conductivity using the relationship between the electrical and the thermal conductivities to be $\lambda_{cyl} = 394$ W/(m K). A 3D heat conduction calculation with *Fluent* has shown that the temperature profile is very close to a one dimensional temperature profile in the upper part of the copper cylinder. Hence, the assumption of a one dimensional temperature profile can be used to calculate the dissipated heat flux based on the three temperature measurements and their distance. The surface temperature is extrapolated using the measured temperature at the thermocouple closest to the surface and the calculated heat flux. Additionally, the temperature and the pressure inside the spray chamber are monitored, as well as the temperatures, of the working fluid in the reservoir and just in front of the nozzle.

The spacing between heater surface and nozzle can be varied between 20 mm and 100 mm. For spacings larger than ≈25 mm, only a fraction of the spray hits the heater, while for smaller distances the total spray volume flux is deposited on the heater.

2.2. Micro structured surfaces

The heat transfer performance of three different surfaces with micro pyramids as surface structures has been compared to that of a smooth polished surface. The surface structures differ in height and width of the pyramids. The dimensions of the structures can be inferred from Table 1. All surface structures were machined into the end face of copper cylinders. One of the surfaces is shown exemplarily in Fig. 3. All structures investigated caused an increase in surface area compared to the smooth surface by a factor of $\sqrt{2}$. The surface roughness of the smooth polished surface was found to be $R_a < 0.3$ μm using a perthometer. The structured surfaces were fixed in their holders such that the bottom of the structures was on the same level as the edge of the conical holder.

One set of calibrated thermocouples is used for each copper cylinder. The thermocouples were checked for

Table 1
Dimensions of surface structures

Structure	Height (in μm)	Width (in μm)
S1	75	150
S2	150	300
S3	225	450

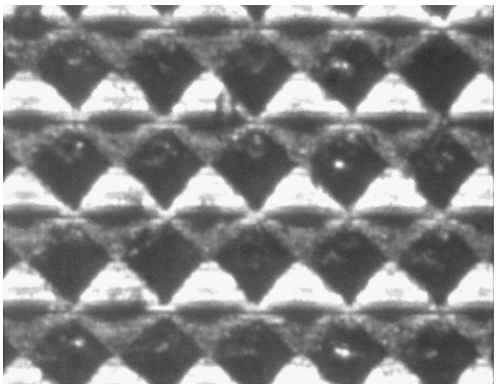

Fig. 3. Top view of micro structured surface (pyramids).

range of temperatures between 25 °C and 60 °C to deviate less than $\Delta t = 0.05$ K from each other in order to minimize the error in the heat flux calculation. The temperatures measured during the experiments were in a range from 30 °C to 55 °C.

2.3. Infrared images

The aforementioned high speed infrared imaging system has been used to obtain images of the coolant behavior on the smooth unstructured copper heater. The emissivity of water differs strongly from that of copper so that information what portion of the heater surface is covered with a water film and where that film is ruptured can be easily extracted from the infrared images. As shown in Fig. 1, the images were taken from the side under an observation angle of ≈60°. Optical access to the heater was permitted by using an infrared transmissive CaF_2-window. The images were taken with a frame rate of 300 Hz. The spatial resolution of the camera system was 100 μm × 100 μm/pixel. Using the Matlab-image processing toolbox, the infrared images were converted to binary matrices consisting of ones where the heater surface is covered with water and zeros elsewhere. The distortion of the images caused by the viewing angle was removed as well by an algorithm which deskews the elliptical image of the circular heater face so that the final image shows a circular shape. Afterwards, an edge detection algorithm was used to calculate the surface area of film covered portions of the heater and their perimeter, which corresponds to the three phase contact line length.

2.4. High resolution temperature measurements

To obtain high spatial resolution temperature measurements at a heated surface, the copper cylinder is replaced in some experiments by a thin stainless steel foil heater with thermochromic liquid crystals (TLCs) applied to the lower surface. A schematic of the foil heater and the applied TLCs is shown in Fig. 4. The colourplay of the TLCs is observed from below through the Plexiglas bottom plate

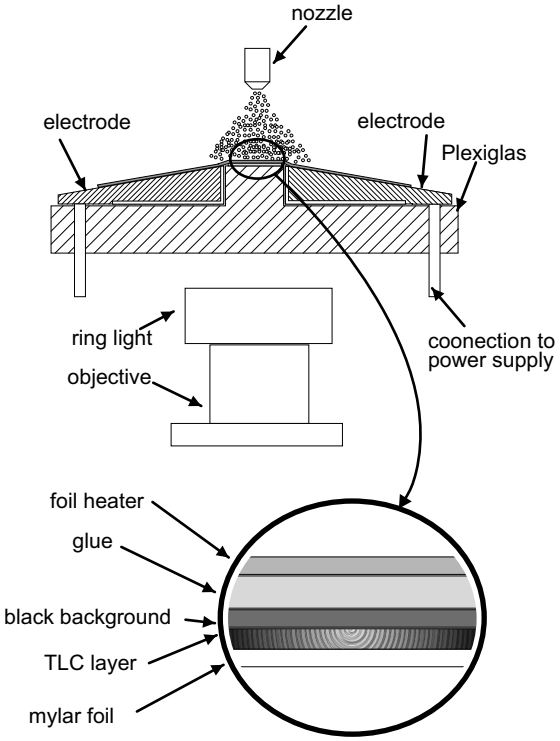

Fig. 4. Schematic of TLC heater.

of the spray chamber with a CCD-camera. The foil heater has a thickness of 10 μm, a 20 μm thick layer of a glue with a high thermal conductivity is used to have a good contact between the backside of the heater and the TLC sheet. The TLC sheet itself consists of 3 layers, a layer of black paint (≈5 μm), a layer of encapsulated TLC (≈240 μm) and a mylar foil as protection (≈125 μm). TLCs reflect a distinct colour depending on their temperature when illuminated by white light. Below and above their active temperature range they are transparent so that the black background can be seen, within their working range the reflected light changes from red to green to blue with increasing temperature. The TLCs used for the current experiment are supplied in the form of a foil such that they are protected from environmental influences. Images of the TLCs are captured using a three chip colour CCD-Camera and the colour information is converted from the RGB-signal of the camera to the HSV-colourspace (Hue, Saturation, Value). In the HSV-colourspace, the hue-value is measured in degrees. It contains all the colour information and can therefore be used as a single value for the temperature measurement. An 'in situ' calibration method for the TLCs has been developed, where the TLCs can be calibrated within the experimental set-up and the temperature of the TLCs can be controlled with a thermostat. A correlation of hue-value and temperature is obtained by measuring the temperature of the TLCs with thermocouples and simultaneously recording their colourplay. A seventh order regression proved to be a good approximation for the

hue-temperature-correlation. The stainless steel foil is electrically heated with constant voltage and current, resulting in a constant heat flow density in the foil. Due to the small thickness of the foil the temperature distribution on the back of the foil does not deviate significantly from that on the front of the foil. The time constant for the measurement system was determined to be $\tau \approx 0.007$ s. The TLCs are illuminated through the Plexiglas base plate of the heater with a ring light, which is connected to a cold light source. The TLC colourplay is acquired with a frame rate of 20 Hz. Thus, the temperature information can only be regarded as snapshots, since the time constant of the foil heater is much smaller than the frame rate. The spatial resolution of the TLC images is 25 μm × 25 μm/pixel. Due to the limited working bandwidth of TLCs (5–20 K), the pressure inside the Plexiglas container has to be controlled such that the saturation temperature of water is well between the limits of the TLC working bandwidth.

2.5. Experimental procedure

Prior to each set of experiments the heater surface is first cleaned with diluted hydrochloric acid, rinsed with deionised water, cleaned with acetone and again rinsed with deionised water. Also, the working fluid water is well degassed before each set of experiments. Then the spray chamber is partly filled with water such that the heat exchanger 2 inside the experimental container (see Fig. 1) is in contact with water. The spray chamber is evacuated to $p_{con} = 0.055$ bar, while the heat exchanger is set to a temperature above the saturation temperature inside the spray chamber so that the water inside the spray chamber evaporates and creates a vapour atmosphere. Also, the temperature of the working fluid in the fluid reservoir is set to $t_{res} = 22$ °C.

The coolant mass flow rate through the nozzle is kept constant at $\dot{m} = 16$ kg/h for all experiments. For this mass flow rate, the droplet diameter was found by PDA measurements to vary between $d_{10} = 40$ μm and $d_{10} = 60$ μm over the spray cone of a TG SS 0.3 nozzle. The mass flux of the spray used for cooling can be varied by varying the nozzle to heater spacing. This way, the spray characteristics remain roughly constant for all volume fluxes. Finally, the cartridge heaters are switched on. When a steady state is reached, data is acquired for 180 s. Afterwards, the power is increased to the next step.

The same nozzle has been used for all experiments and the pressure drop across the nozzle was monitored to be within $\Delta p_{nozzle} = \pm 0.1$ bar throughout all experiments.

3. Results and discussion

In this section the experimental results obtained from the heat performance measurements on the different surface structures are presented and compared, followed by the presentation results of the infrared and the TLC image analysis.

3.1. Spray cooling performance on smooth surfaces

First some general results found for spray cooling on a smooth heater will be presented.

Generally, it can be stated that for a given wall superheat the dissipated heat flux could be increased by decreasing the nozzle spacings. However, it was observed that for some wall superheats, a higher heat flux could be dissipated using a higher nozzle spacing and thus a lower coolant flux. Comparing the data for a smooth surface shown in Fig. 5, it can be seen that for a wall superheat between $\Delta t_w = 4$ K and $\Delta t_w = 6$ K, a higher heat flux can be dissipated with a nozzle spacing of 60 mm than with a spacing of 40 mm. For a nozzle spacing of 60 mm the coolant film on the heater ruptures at a wall superheat $\Delta t_w \approx 3$ K leading to only small increases in Δt_w when the heat flux $\dot{q}$ is increased. At a wall superheat of $\Delta t_w \approx 6$ K, the effect of the higher coolant mass flux becomes dominant again, so that a higher heat flux can be removed with a lower nozzle spacing. Also, for the nozzle spacing of 60 mm, the removed heat flux tends towards the maximum heat flux that can be removed with this coolant mass flux, such that small increases in heat flux lead to large increases in wall superheat.

Thus, in a small region of wall superheats, the dissipated heat flux $\dot{q}$ is higher for the larger nozzle spacing than for lower spacings and the corresponding higher coolant fluxes. A similar behavior was observed for a nozzle spacing of 80 mm.

3.2. Infrared observations

Observations on a smooth heater surface using an infrared camera system allow a distinct determination of the wetted and not wetted heater surface area. Additionally, the three phase contact line (water, vapour, copper) surrounding the wetted area could be easily obtained by

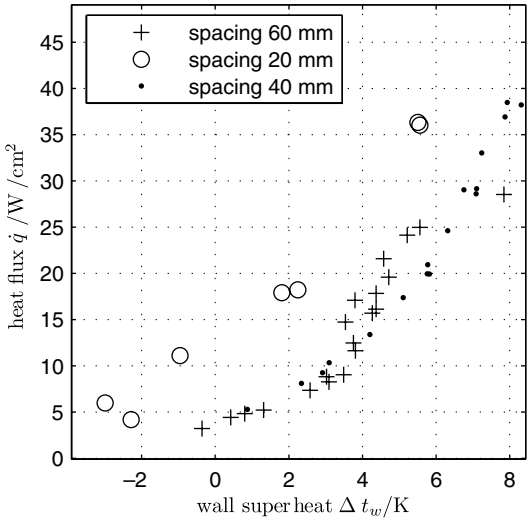

Fig. 5. Spray cooling performance for different nozzle spacings on a smooth surface.

analysing the infrared pictures. A plot of wetted surface area and contact line length versus heat flux is shown in Figs. 6 and 7, where Fig. 7 also shows the corresponding IR-images for different heat fluxes. As can be seen in Figs. 6 and 7, the area of the wetted surface decreases with increasing heat flux, while the contact line length increases almost proportional to the heat flux. This observation compares well to the findings of Kim et al. [9], who performed similar measurements on a transparent heater. Based on this observation, it can be inferred that increasing the three phase contact line length leads to an enhanced cooling performance. Thus, using a structured surface like the pyramid structures S1–S3 at coolant mass fluxes low enough such that the tips of the surface structures protrude out of the coolant film should lead to an improved cooling performance in terms of wall superheat at a given heat flux.

3.3. Spray cooling performance on micro structured surfaces

The spray cooling performance of heaters with different surfaces geometries has been investigated for different nozzle spacings. The results have been compared to the spray cooling performance of a smooth polished surface using the same spray nozzle.

For the spray cooling on the surface with the smallest structures (S1), no significant difference in the spray cooling performance compared to the smooth surface could be observed until a certain wall superheat was reached. At this wall superheat, the coolant film ruptured and the capillary forces of the structure are believed to have drawn the coolant into the structure such that the upper parts of the surface structure protruded out of the coolant film. Hence, the contact line length was increased and a strong reduction in wall superheat was observed, despite an increased heat flux. This behavior could be observed for larger to intermediate nozzle spacings. For very low nozzle spacings, no effect of the surface structure S1 could be observed within the wall superheat range investigated. A plot of heat flux versus wall super heat for two different nozzle spacings is shown in Fig. 8. As can be seen, for a wall superheat of approximately $\Delta t_w = 1$ K a higher heat flux can be dissipated when the nozzle spacing is larger and the coolant mass flux is lower. Also, the aforementioned characteristic reduction in wall superheat can be observed for both nozzle spacings.

As shown in Fig. 9, the jump towards lower wall superheat Δt_w with increasing heat flux can only be observed for the largest nozzle spacing in case of the surface with the largest structures investigated (S3). Infrared images taken during the spray cooling experiments with a nozzle spacing of 60 mm show that the tips of the micro pyramids protrude out of the coolant film for every wall superheat investigated, thus enhancing the heat transfer also for lower heat fluxes. For the surface structure with the intermediate structure size (S2), a characteristic reduction in the temper-

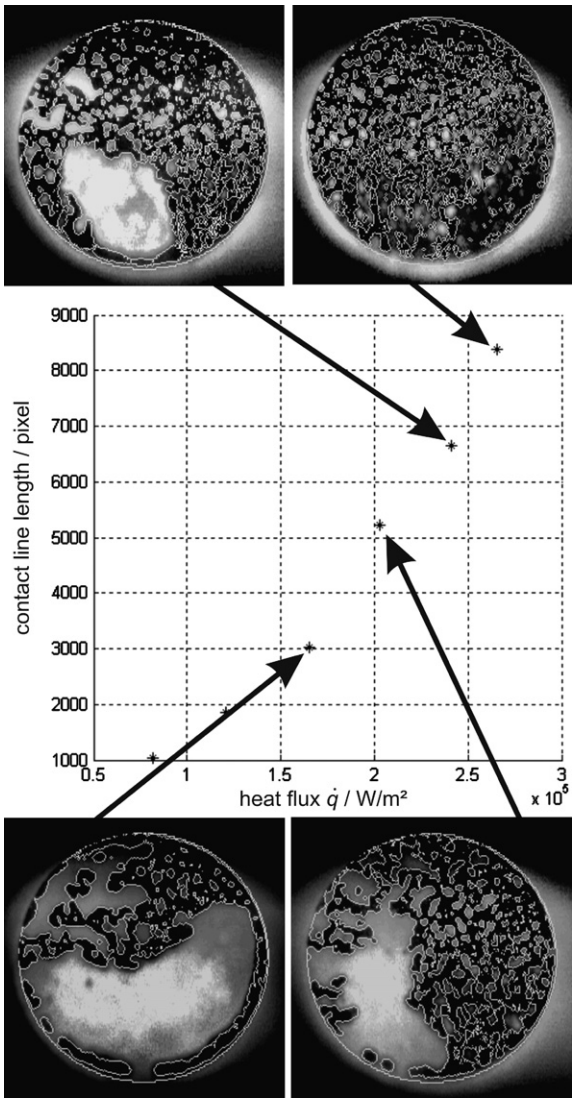

Fig. 7. Contact line length versus heat flux with corresponding IR-images.

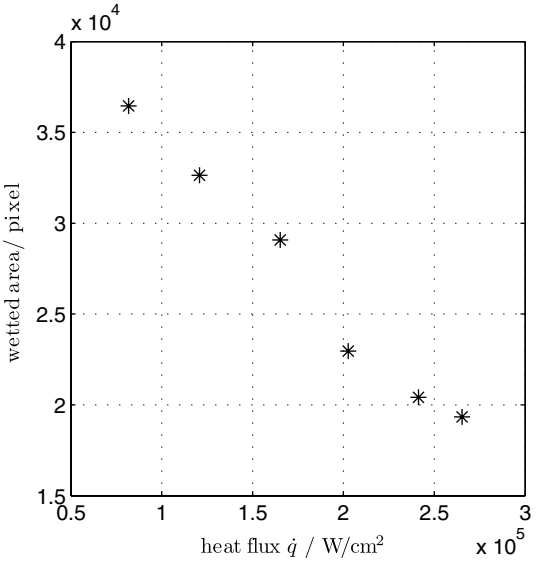

Fig. 6. Wetted area versus heat flux.

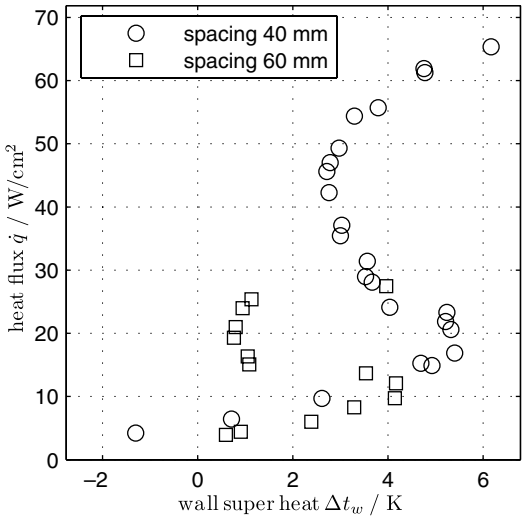

Fig. 8. Spray cooling performance on surface S1.

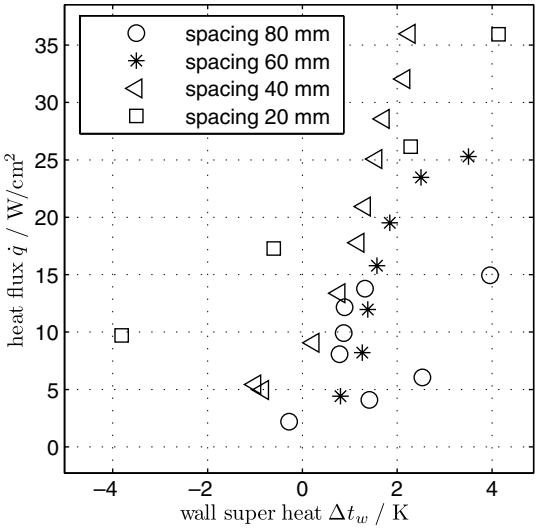

Fig. 9. Spray cooling performance on surface S3.

ature could be observed. However, this temperature jump occurred at lower wall superheats and lower heat fluxes than for the surface structure (S1) as can be seen in Fig. 10.

A comparison of the spray cooling performance on the three surface structures investigated and on the smooth surface is shown in Fig. 10. The nozzle spacing for all measurements was 60 mm. As can be seen from the figure, there is a significant enhancement in heat transfer due to the surface structures. For the surface structure S3 an increase in heat flux with a factor of 2–5 can be obtained for a wall superheat in the range of $\Delta t_w = 2$–3 K. Also, the gradient $\frac{d\dot{q}}{d\Delta t_w}$ is significantly larger for structured surfaces. The steepest gradient was observed when the surface structure S1 was used. A steep gradient is advantageous from an application point of view, since the wall temperature can be kept fairly constant over a broader range of heat fluxes.

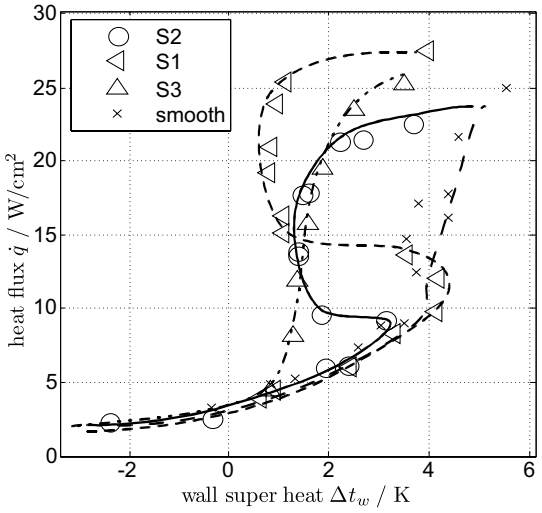

Fig. 10. Comparison of spray cooling on different surfaces (nozzle spacing 60 mm).

3.4. High resolution temperature measurements

For a first evaluation of the temperature distribution underneath a flat spray cooled surface, two different conditions have been studied. In both conditions, the spacing between nozzle and heater was sufficiently large so that the heater was well within the spray cone. The first condition corresponds to the low heat flux, low surface superheat regime, where the heater is fully covered with a water film. In this case, comparatively small temperature gradients underneath the surface could be observed. A typical temperature profile for this regime is shown in Fig. 11.

The second condition investigated is that of a ruptured film on the heater, which usually occurs for higher heat fluxes and wall superheats. The ruptured film results in higher temperature gradients. The hotter areas correspond to the areas covered with the fairly thick liquid, while the film is ruptured in the colder areas and the small spray

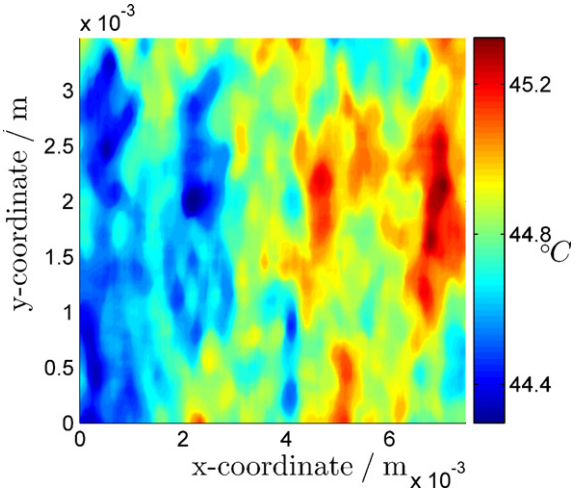

Fig. 11. Temperature distribution under spray cooled surface.

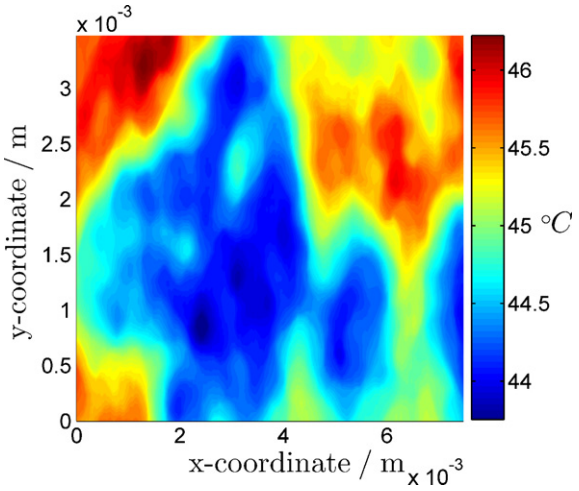

Fig. 12. Temperature distribution beneath ruptured spray film.

droplets can directly evaporate on the heater or agglomerate with other droplets to form larger wetted areas. The lower temperatures beneath the ruptured film clearly indicates that the direct evaporation of spray droplets leads to a better heat transfer. The drawback of this regime are higher temperature gradients. A typical temperature distribution for this regime is shown in Fig. 12. While the temperature beneath the heater completely covered with a coolant film varies by approximately 1 K, the temperature beneath the heater only partly covered with a coolant film varies by more than 2 K. By comparing Figs. 11 and 12 it becomes obvious that the temperature gradients below the ruptured coolant film are significantly larger than below the cohesive coolant film. In case of the ruptured film, higher temperatures are observed beneath agglomerated water. While the droplets from the spray nozzle evaporate comparatively fast if they get in direct contact with the heater and hence lead to a good heat transfer, agglomerated droplets lead to a thicker water layer with a higher thermal resistance.

While such small temperature variations have been observed for large nozzle spacings, for smaller distances, when the heater was only partly covered by the spray cone, high temperature gradients occurred at the edges of the spray cone, such that the temperature difference between the middle of the spray cone and its edge was found to exceed 18 K. A plot of the temperature distribution below the heater surface from the middle of the spray cone towards its edge is shown in Fig. 13. Thus, the results obtained for small nozzles spacings have some similarity to the temperature variations found by Shedd and Pautsch [12], while for larger nozzle spacings small temperature variations have been found as observed by Gu et al. [11]. No significant influence of the nozzle spacing on the temperature variations were found once the heater was completely inscribed in the spray cone.

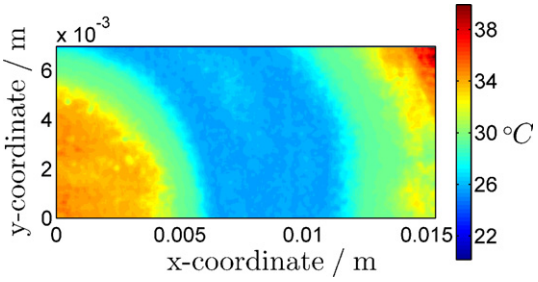

Fig. 13. Temperature distribution for low nozzle spacing.

4. Conclusion

The experiments have shown that spray cooling on micro structured can lead to significantly improved cooling performances compared to smooth surfaces at the same wall superheat. The authors believe this effect is due to an increased length of the three phase contact line that forms on the structures which leads to a very efficient thin film evaporation. Using an infrared camera, it could be shown that for a smooth surface the dissipated heat flux increases with increasing contact line length, which occurs on a smooth surface when the coolant film covering the surface at low surface superheats ruptures. Additionally, it could be shown that the temperature distribution shows stronger temperature gradients when the coolant film ruptures. Also, small nozzle spacings lead to large temperature gradients on the heater surface.

Acknowledgements

The authors wish to acknowledge the support of the German Research Foundation (DFG) via the Emmy-Noether-Program.

References

[1] J. Yang, L. Chow, M. Pais, Nucleate boiling heat transfer in spray cooling, ASME J. Heat Transfer 118 (1996) 668–671.
[2] S. Toda, A study of mist cooling (1st Report: investigation of mist cooling), Heat Transfer – Jpn. Res. 2 (1972) 39–50.
[3] I. Mudawar, W. Valentine, Determination of the local quench curve for spray-cooled metallic surfaces, J. Heat Treating 7 (1998) 107–121.
[4] I. Mudawar, K. Estes, Optimizing and predicting CHF in spray cooling of a square surface, ASME J. Heat Transfer 118 (1996) 672–679.
[5] A. Pautsch, T. Shedd, G. Nellis, Thickness measurements of the thin film in spray evaporative cooling, in: Proc. of Thermal and Thermomechanical Phenomena in Electronic Systems, ITHERM '04, vol. 1, 2004. pp. 70–76.
[6] J. Yang, L. Chow, M. Pais, Liquid film thickness and topography determination using fresnel diffraction and holography, Exp. Heat Transfer 5 (1992) 239–252.
[7] M. Sehmbey, M. Pais, L. Chow, Effect of surface material properties and surface characteristics in evaporative spray cooling, J. Thermophys. Heat Transfer 6 (1992) 505–512.
[8] C. Hsieh, Y. Yao, Heat Transfer of water sprays on enhanced silicon surfaces, in: Proc. 12th Int. Heat Transfer Conf., Grenoble, 2002.

[9] E. Silk, J. Kim, K. Kiger, Investigation of enhanced surface spray cooling, in: Proc. of IMECE 2004, Anaheim (USA), 2004.
[10] B. Horacek, J. Kim, K. Kiger, Single nozzle spray cooling heat transfer mechanisms, Int. J. Heat Mass Transfer 48 (8) (2005) 1425–1438.
[11] C.B. Gu, G.S. Su, L.C. Chow, M.R. Pais, Comparison of Spray and Jet Impingement Cooling, ASME Paper, 93-HT-20, 1993.
[12] T.A. Shedd, A.G. Pautsch, Spray impingement cooling with single- and multiple nozzle arrays. Part II: Visualization and empirical models, Int. J. Heat Mass Transfer 48 (2005) 3176–3184.
[13] J.R. Rybicki, I. Mudawar, Single-phase and two-phase cooling characteristics of upward-facing and downward-facing sprays, Int. J. Heat Mass Transfer 49 (2006) 5–16.